

Magnetic properties of monodispersed Co/CoO clusters

D. L. Peng,* K. Sumiyama, T. Hihara, S. Yamamuro, and T. J. Konno

*Institute for Materials Research, Tohoku University, 2-1-1 Katahira, Aoba-ku, Sendai 980-8577, Japan
and CREST of Japan Science and Technology Corporation, Kawaguchi 332-0012, Japan*

(Received 28 July 1999)

Monodispersed Co/CoO cluster assemblies with the mean cluster sizes of 6 and 13 nm have been prepared by a plasma-gas condensation type cluster beam deposition apparatus. We measured the effects of the oxygen gas flow rate during deposition, temperature, and cluster size on the coercivity and hysteresis loop shift induced by field cooling. The large exchange bias field (10.2 kOe) and coercivity (5 kOe) were observed at 5 K for the monodispersed Co/CoO cluster assembly with $d=6$ nm. The correlations between unidirectional anisotropy and uniaxial anisotropy, training effect and magnetic relaxation can be interpreted by the hypothesis of a spin disorder in the interfacial layer between the antiferromagnetic CoO shell and the ferromagnetic Co core.

I. INTRODUCTION

We have recently developed the plasma-gas-condensation (PGC) type cluster beam deposition apparatus, which is a combination of sputtering and condensation in an inert gas atmosphere.¹ Using this system, we have succeeded in obtaining monodispersed transition-metal clusters with the mean sizes $d=6$ to 15 nm and the standard deviation less than 10% of d . In this cluster-size range, the characteristic percolation during the assembling process suggests considerable distribution in the cluster connectivity.² In order to stabilize the cluster surface, we have uniformly oxidized Co cluster surface, because the melting point of CoO is very high. In the core-shell type Co/CoO monodispersed cluster assemblies thus obtained, characteristic tunnel-type conductivity and enhanced magnetoresistance, arising from the uniform Co core size and CoO shell thickness, have been reported.^{3,4} In this paper, we focus our attention on magnetic properties of the monodispersed Co/CoO cluster assemblies.

Unidirectional exchange anisotropy (UEA) was first discovered in field-cooled Co/CoO particles⁵ more than 40 years ago and shown to be caused by the strong exchange coupling between the ferromagnetic (FM) Co core and the antiferromagnetic (AF) CoO layer. The typical UEA effect is a marked shift of the hysteresis loop against the applied field, commonly referred to as an exchange bias field, H_{eb} , when field cooling the sample from temperatures above the Néel temperature T_N of the AF to $T < T_N$. The related phenomena have been studied theoretically⁶⁻⁹ and experimentally,¹⁰⁻¹⁷ because they are technologically important to domain stabilizers in magnetoresistive heads¹⁸ and spin-valve-based devices.¹⁹ However, the understanding of the UEA effect has not been well-understood because it is very difficult to determine the AF spin structures in interfacial layer contributing to H_{eb} . The first simple model⁵ dealt with the unidirectional anisotropy by assumption of a perfect uncompensated plane of the AF at the interface and predicted H_{eb} , which was two orders of magnitude larger than the observed ones. Mauri *et al.*⁶ explained the small experimental value of H_{eb} by assuming the formation of a domain wall parallel to the interface which dramatically lowers the energy required to reverse the magnetization. Alternatively, Koon⁸ predicted a

correct value for H_{eb} as a result of a perpendicular orientation between the FM and AF axes, similar to the classical spin-flop state in bulk AF. The recent polarized neutron diffraction experiment has shown that exchange coupling between the Co and CoO layers is apparently responsible for the increased projection of the AF moments perpendicular to the cooling field direction.¹⁴ Although the theoretical models have mainly explained the unidirectional anisotropy and obtained the correct order of H_{eb} , they have predicted no effect on the coercivity H_c . Experimentally, the shifted hysteresis loop is always accompanied by an enhancement of the coercivity, which is much larger than the intrinsic value of the ferromagnetic (FM) core^{5,11} and layer.¹⁰ Quite recently, Schulthess and Butler⁹ have made a calculation for CoO/FM films using an atomistic Heisenberg model and have shown that there are two coupling mechanism at work, the spin-flop coupling (being responsible for a large coercivity) and FM-AF coupling through uncompensated defects (accounting for exchange bias field).

For the small CoO-coated Co clusters, magnetic reversal mechanism, real roughness and spin structures at core-shell interface should be different from that for simple FM/AF bilayers because of single-domain structure of Co core grains and the small size of cores and shell crystallites. The present work explores the correlation between unidirectional anisotropy and uniaxial anisotropy, training effect and the magnetic relaxation to be related to magnetization reversal mechanism in the monodispersed Co/CoO cluster assemblies. We describe the influence of the cluster size, surface oxidation extent and temperature on H_{eb} and H_c . Finally, we also mention the magnetic relaxation behavior in the Co/CoO cluster assembly.

II. EXPERIMENT

The samples were prepared by the PGC-type cluster beam deposition apparatus, whose detail was described elsewhere.¹⁻³ We introduced oxygen gas through a nozzle set near the skimmer into the deposition chamber to form cobalt-oxide shells covering the Co clusters before depositing on the substrate. This process ensures that all Co clusters are uniformly oxidized before the cluster assemblies are

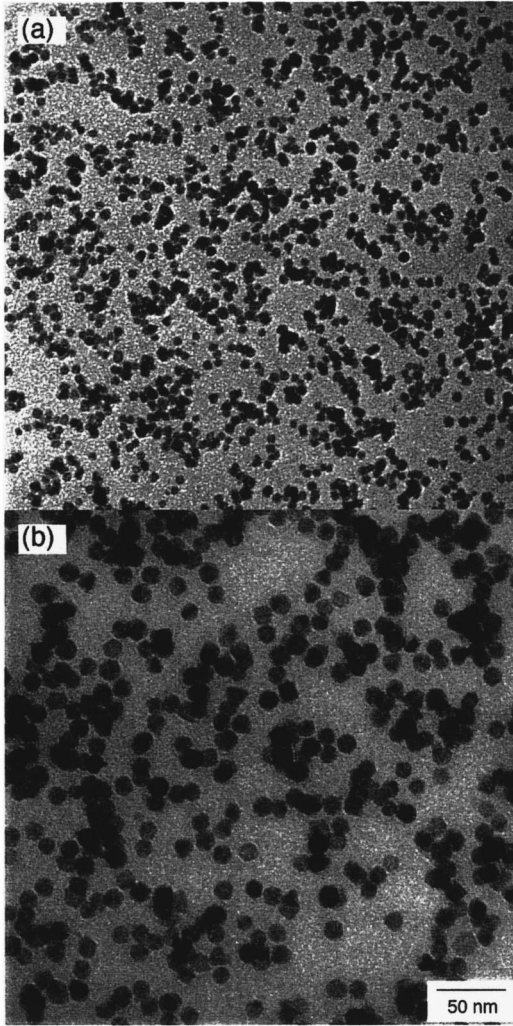


FIG. 1. TEM images of the monodispersed Co/CoO clusters prepared on a carbon microgrid at the O_2 gas flow rate $R_{O_2}=1$ SCCM. (a) Mean cluster diameter $d=6$ nm and (b) $d=13$ nm.

formed.⁴ For constant R_{Ar} or $R_{Ar}+R_{He}$, the gas pressure in the deposition chamber can be adjusted lower than 3×10^{-4} Torr by changing the flow rate of oxygen gas (R_{O_2}). We can control the cluster size by changing R_{Ar} and R_{He} . Figure 1 shows transmission electron microscopy (TEM) images of the initial stage of the oxide-coated Co cluster assemblies prepared at $R_{O_2}=1$ SCCM. As shown here, the clusters are almost monodispersed, with the mean diameter d of about (a) 6 and (b) 13 nm. The electron diffraction pattern clearly indicated coexistence of fcc Co and CoO phases, while the high-resolution transmission electron microscope image displayed that the Co clusters were covered with the CoO shells composed of very small crystallites.⁴ The cluster assemblies were formed on a polyimide film at room temperature with the apparent thickness of about 100 nm, as measured by a quartz thickness monitor. Magnetic measurement was performed using a superconducting quantum interference device magnetometer between 5 and 400 K with the maximum field of 50 kOe.

III. RESULTS

A. Unidirectional anisotropy and uniaxial anisotropy

Hysteresis loops were measured at 5 K after zero-field cooling (ZFC) and field cooling (FC) the samples from 300 to 5 K in a magnetic field H of 20 kOe. The direction of H used to measure the loops was parallel to that of the cooling field. Figure 2 shows the ZFC and FC loops of the Co/CoO monodispersed cluster assembly with $d=6$ nm prepared at $R_{O_2}=1$ SCCM. For this sample, the thickness of the CoO shell have been estimated to be about 1 nm by direct observation of the high-resolution transmission electron microscope, being consistent with the Co core size of about 4 nm estimated from the Langevin fitting to the experimental data above room temperature. The large H_{eb} ($=|H_1^{FC}+H_2^{FC}|/2$) value of 10.2 kOe is detected, which indicates presence of strong UEA in the present specimen. The large coercivity H_c ($=|H_1^{ZFC}-H_2^{ZFC}|/2 \approx 5$ kOe) is also obtained for the ZFC case in which the UEA effect is randomized. As seen in the inset of Fig. 2, H_{eb} increases with increasing the cooling field and almost becomes unchanged when the cooling fields are higher than 10 kOe. This indicates that the UEA is enhanced with increasing the cooling field in the low-field range.

Figure 3 shows the effect of R_{O_2} on H_c and H_{eb} for the Co/CoO cluster assemblies with $d=6$ and 13 nm. For both cases, H_c and H_{eb} firstly increases with increasing R_{O_2} and then becomes unchanged for $R_{O_2}>1$ SCCM, probably because the oxidation is decelerated and reaches a stable state in the low- O_2 pressure atmosphere ($<3 \times 10^{-4}$ Torr). The increases of H_c and H_{eb} are attributable to the increase of the exchange interaction between the FM Co cores and AF CoO shells because their volume fractions change with R_{O_2} . Moreover, it should be noted that H_c rapidly increases with increasing R_{O_2} for $d=6$ nm, being up to about 5 kOe at $R_{O_2} \geq 1$ SCCM. This H_c value is much larger than that of Ag-coated Co particles (500–2000 Oe for $d=5-13$ nm).¹¹ These results indicate that the uniaxial anisotropy is enhanced by the exchange interaction.

Figures 4(a) and 4(b) show H_c and H_{eb} as a function of temperature for the Co/CoO cluster assemblies with $d=6$ and 13 nm prepared at $R_{O_2}=1$ SCCM. The temperature dependence of H_c is different from that of H_{eb} . H_c does not change markedly at low temperature and then decreases rapidly with increasing temperature above 100 K, while H_{eb} rapidly decreases with increasing temperature and becomes undetectable above $T_v=200$ K, where T_v is much lower than the Néel temperature ($T_N=293$ K) of the bulk CoO. The temperature dependence of H_{eb} indicates that UEA disappears at about 200 K. A similar result observed for oxide passivated Co fine particles was attributed to the superparamagnetic behavior of the AF oxide shell with very small crystallites above a blocking temperature (150 K).¹¹ The superparamagnetism of small AF particles is associated with uncompensated surface spin. However, taking into account of the roughness of core-shell interfaces as well as the small sizes of the Co cores and CoO shell crystallites, the disappearance of the loop shift above 200 K for the CoO-coated

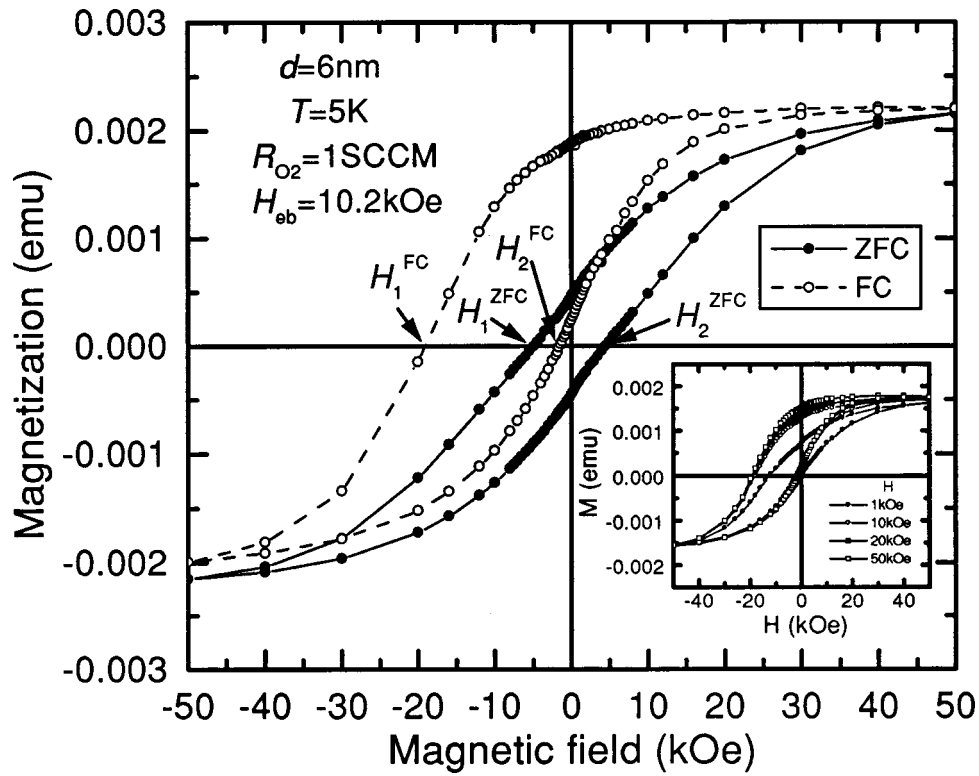


FIG. 2. Hysteresis loops of the zero-field cooled (ZFC) and field-cooled (FC) Co/CoO monodispersed cluster assembly with mean cluster size of $d = 6$ nm prepared at the O_2 gas flow rate $R_{O_2} = 1$ SCCM. The inset shows hysteresis loops after field cooling the sample in different magnetic fields.

Co cluster assemblies should be due to spin disorder at and near core-shell interface. This results in the strong temperature dependence of the anisotropy for the interfacial layer of the AF CoO.

Figure 5 shows the ZFC and FC magnetization as a function of temperature from 390 to 5 K for the monodispersed Co/CoO cluster assembly with $d = 6$ nm. The low field ($H = 100$ Oe) thermomagnetic curves show the following dis-

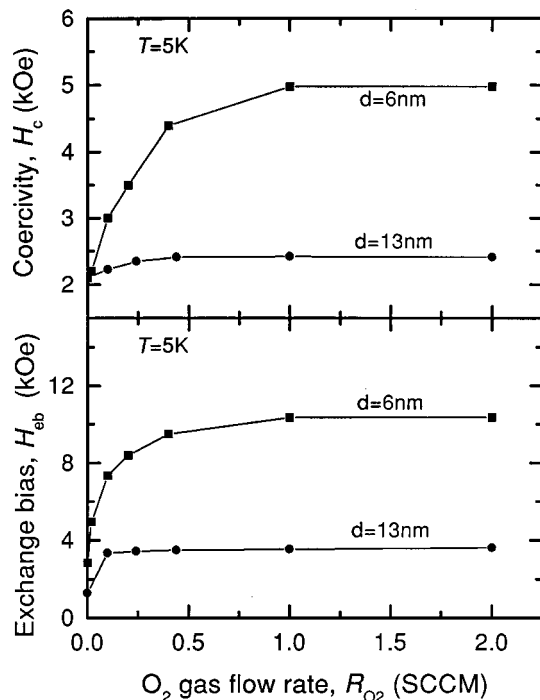


FIG. 3. Coercivity H_c and exchange bias field H_{eb} at 5 K as a function of the O_2 gas flow rate R_{O_2} for the Co/CoO cluster assemblies with $d = 6$ nm and 13 nm.

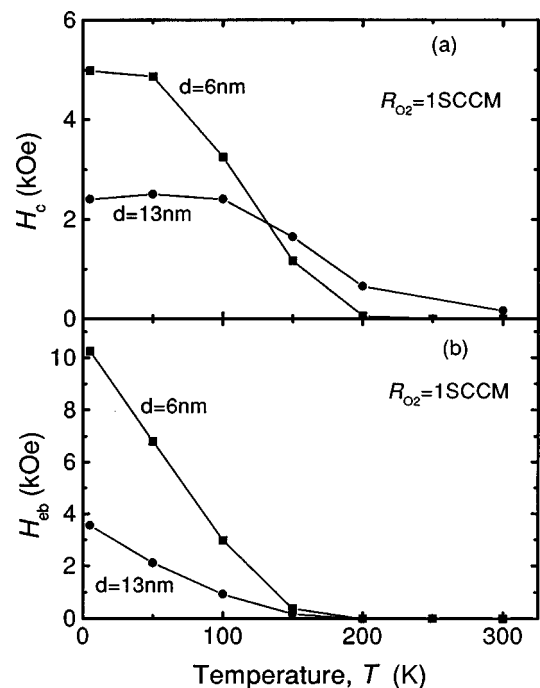


FIG. 4. Temperature dependence of (a) H_c and (b) H_{eb} for the Co/CoO cluster assemblies with $d = 6$ and 13 nm prepared at different $R_{O_2} = 1$ SCCM.

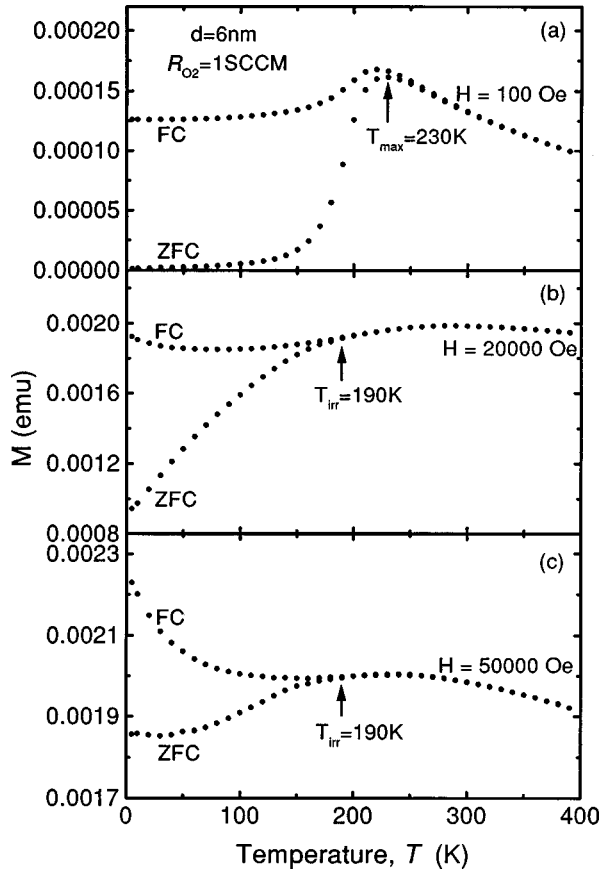


FIG. 5. ZFC and FC magnetization as a function of temperature from 390 to 5 K for the monodispersed Co/CoO cluster assembly with $d=6$ nm. The measuring field is the same with the cooling field. (a) $H=100$, (b) 20 000 and (c) 50 000 Oe.

tinct features [Fig. 5(a)]. The ZFC magnetization is almost zero and the FC magnetization unchanged below 150 K because of the strong exchange coupling between the Co core and CoO shell. Both ZFC and FC magnetization curves rapidly increase with temperature above 150 K and reveal a maximum at $T_{\max}=230$ K. This behavior indicates that UEA starts to decrease rapidly with increasing temperature above 150 K. For the high field ($H=20\,000$ and $50\,000$ Oe) thermomagnetic curves [Figs. 5(b) and 5(c)], the ZFC magnetization is seen to increase with increasing temperature and to coincide with the FC magnetization at $T_{\text{irr}}=190$ K (corresponding to starting temperature of irreversibility). It is noteworthy that T_{irr} do not decrease with increasing the external field at the high field range and roughly coincides with T_v . This indicates that the exchange interaction is different from conventional dipole interaction between FM clusters: T_{irr} and T_v are mainly determined by the anisotropy of the AF CoO shell rather than the intrinsic anisotropy of the Co core.

B. Training effect

In order to investigate the dependence of the exchange bias field H_{eb} on repeated magnetization reversals, namely the so-called training effect, the monodispersed Co/CoO cluster assembly with $d=6$ nm was measured at 5 K using a superconducting quantum interference device (SQUID) magnetometer. The training effect is a diminution of H_{eb} upon

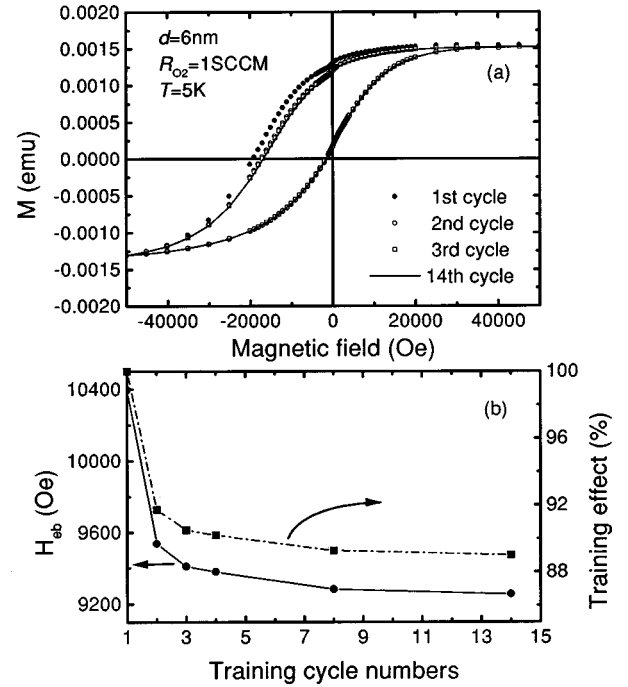


FIG. 6. (a) Successive hysteresis loops measured at 5 K along the easy axis after cooling from 300 K in a field of +20 000 Oe along the same direction; (b) H_{eb} and training effect as a function of the training cycle number for the monodispersed Co/CoO cluster assembly with $d=6$ nm.

the subsequent magnetization reversals.¹⁰ Figure 6(a) shows typical results for the loops obtained along the field-cooling direction at 5 K. The successive loops do not coincide with each other and show a decrease in H_{eb} . Figure 6(b) shows the dependence of H_{eb} and the training effect on the training cycle number at 5 K. Here, we define the training effect as the fraction of the initial value, which is lost after field cycling. The decrease of H_{eb} is larger for the second cycle and then become unchanged after further numbers of the training cycles. The training effect is about 89% after the 14th cycle.

C. Magnetic relaxation phenomenon

Magnetic relaxation measurements were performed for the Co/CoO cluster assembly using the following procedure: first the sample was cooled from 300 K to a lower temperature in low magnetic field, $H_a=100$ Oe; the field was then reversed to $H_b=-100$ Oe and the variation of the magnetization with time was measured at this temperature. As shown in Fig. 7, the magnetic relaxation follows logarithmic time dependence:²⁰

$$M(t) = M(t_0)[1 - S(T)\ln(t/t_0)], \quad (1)$$

where S is the magnetic viscosity and t_0 the fitting parameter. There is no single exponential time dependence as expected for a collection of identical, noninteracting single domain clusters aligned in the same direction by a field (i.e., the anisotropy energy barrier is universal throughout the system). This implies a wide distribution of the anisotropy energy, which is ascribed to polycrystalline CoO and different interfacial state in spite of the narrow cluster size distribution. By least square fitting of Eq. (1) to the results in Fig. 7,

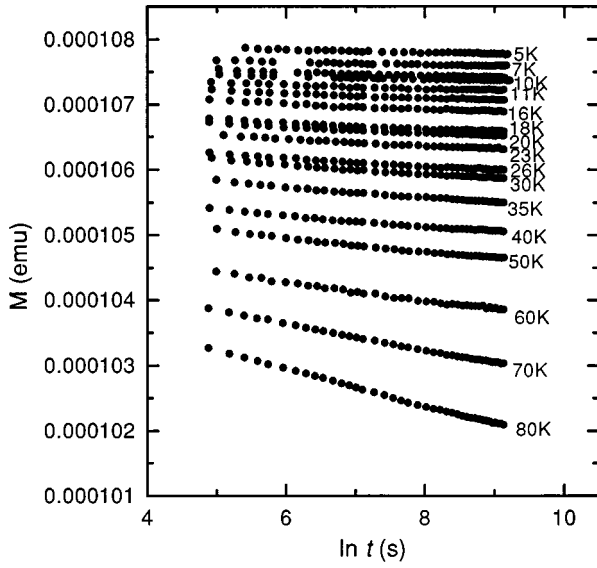


FIG. 7. Time dependence of magnetization at different temperatures for the Co/CoO monodispersed cluster assembly with $d = 6$ nm prepared at $R_{O_2} = 1$ SCCM.

the S value is estimated as a function of temperature and shown in Fig. 8. The temperature variation of S at a high temperature range deviates from linearity. However, for $8 < T < 50$ K, S varies linearly with T , extrapolating to zero when $T = 0$, as would be expected for the magnetic relaxation via thermal activation. This indicates that the interaction between the Co cores is smaller than the energy barrier height, probably because the dipole interaction between the Co cores is shielded partially by the AF CoO shell.

The other remarkable feature is that the S values are independent of temperature at $T \leq 8$ K. Such a nonthermal relaxation character below a few Kelvin has been observed in several nanostructured materials with the broad distribution of sizes or anisotropy energy barriers,^{21–24} being ascribed to a macroscopic quantum tunneling (MQT) effect of magnetization. The MQT effect is observable at experimentally ac-

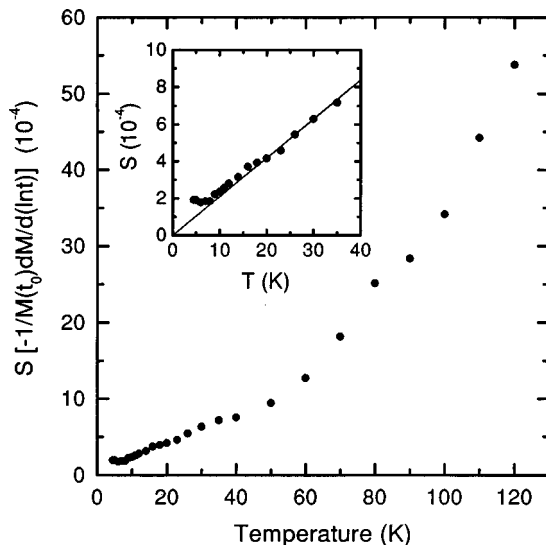


FIG. 8. Magnetic viscosity S as a function of temperature for the Co/CoO monodispersed cluster assembly with $d = 6$ nm prepared at $R_{O_2} = 1$ SCCM.

cessible temperatures only for materials with high uniaxial anisotropy. Indeed, for the present Co/CoO cluster assembly, $H_c = 5$ kOe (see Fig. 2) and the uniaxial anisotropy constant, $K \approx H_c \times M_s \approx 7.2 \times 10^6$ erg/cm³, which is larger than the bulk value ($K = 4.5 \times 10^6$ erg/cm³ and 2.5×10^6 erg/cm³ for bulk hcp and fcc Co, respectively).²⁵ Therefore, the high crossover temperature from a thermal activation regime to a quantum tunneling regime, $T_c^* = 8$ K, is ascribed to the enhanced uniaxial anisotropy due to exchange coupling between the FM Co core and AF CoO shell.

IV. DISCUSSION

As described in Sec. III A, there is strong correlation between H_{eb} and H_c . The large coercivity ($H_c = 5000$ Oe) is detected for the Co/CoO cluster assembly with $d = 6$ nm. It is impossible that such enhancement of H_c results from magnetic interaction between the FM Co cores. Clearly, the enhancement of H_c mainly stems from the UEA effect. Recently, the correlation between H_{eb} and H_c have been discussed for the Parmalloy/CoO bilayers^{16,17} as a theoretical extension of Malozemoff's model.⁷ The UEA effect is interpreted in terms of random exchange fields due to roughness and imperfection at the FM and AF interface, giving the correct order of magnitude for H_{eb} . Here, we discuss the correlation between H_{eb} and H_c for small Co/CoO cluster assemblies. Figure 9 shows coercivities, H_c and H_c^{FC} ($= |H_1^{FC} - H_2^{FC}|/2$), of the ZFC and FC samples at 5 K as a function of H_{eb} for the monodispersed Co/CoO cluster assemblies with $d = 6$ and 13 nm prepared at different R_{O_2} . Both H_c and H_c^{FC} increase with the increase of H_{eb} , indicating the clear correlation between H_{eb} and H_c . Comparing the case of $d = 6$ nm with that of $d = 13$ nm, the size reduction of the Co core is more important for the increase in H_c although the increase in H_{eb} can be correlated with both the increase in the CoO layer thickness and the decrease in the Co core size.¹⁷ It is noteworthy that the value of H_c^{FC} is about twice as large as that of H_c at a given H_{eb} value. This fact

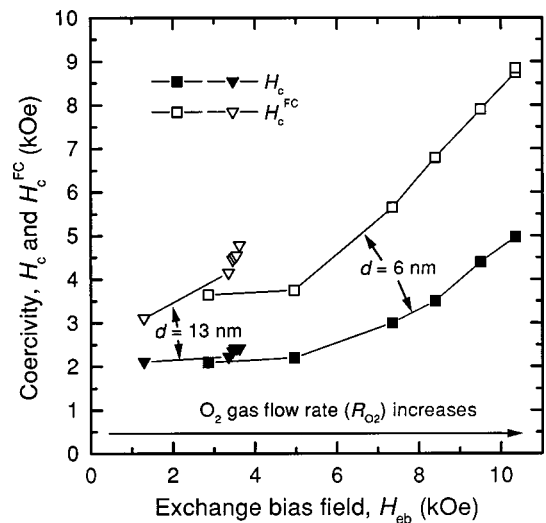


FIG. 9. Coercivities, H_c and H_c^{FC} of the ZFC and FC samples at 5 K as a function of the exchange bias field H_{eb} for the Co/CoO monodispersed cluster assemblies with $d = 6$ and 13 nm prepared at different R_{O_2} .

suggests that a magnetization reversal mechanism of rotation exists and a uniaxial anisotropy is parallel to UEA. Although there is microscopically UEA in a ZFC single-domain particle system with a FM-AF core-shell interface, it is macroscopically smeared out by the random orientation of the single-domain cores.⁵ However, the presence of the uniaxial anisotropy of these single-domain Co cores gives a H_c value. When the sample is cooled in a high external field across the Néel temperature of the AF shell, the magnetic moments of the Co cores are oriented in the cooling field direction and blocked at low temperatures. Then, finite H_{eb} and large H_c^{FC} (about twice of H_c) are expected when the loop measurement is carried out along the cooling field.

With regard to the origin of the enhanced coercivity or uniaxial anisotropy for the FM/AF particle or bilayer systems, there are mainly the following interpretations: (1) presence of spin disorder state, similar to spin glass, at and near the FM/AF interface;^{10,26} (2) pinning of the domain walls in the FM layer by local-energy minima created by the random interaction field with the AF layer;¹⁷ (3) the spin-flop coupling at the FM/AF interface.⁹ For the small CoO-coated Co clusters, spin orientation at and near core-shell interface are different from that for simple FM/AF bilayers because of the small size of cores and shell crystallites. For example, Mössbauer spectroscopy study on surface oxidized Fe nanoparticles revealed that the surface shell consisted of very small crystallites and that a large spin canting characterized the oxide phase.²⁷⁻²⁹ Kodama *et al.*³⁰ has also observed the spin canting at the surface of nickel ferrite nanoparticles. This is due to reduced coordination and broken exchange bonds between surface spins, being compatible with a spin-glass-like behavior at the surface. The first origin mentioned above, namely the hypothesis of spin disorder at and near the FM core and AF shell interface, is applicable for the present monodispersed Co/CoO cluster assemblies. According to this hypothesis, UEA almost disappears at freezing temperature T_g . $T_g = T_v = 200$ K, being much lower than the Néel temperature ($T_N = 293$ K) of the bulk CoO. The application of a field at temperature higher than T_g forces the Co cores to lie along the field direction. Owing to the exchange coupling, the presence of the surface frozen spins favors the FM Co core to be magnetized in the field-cooling direction, resulting in a shift of the hysteresis loops below T_g . On the other hand, one characteristic of a spin glass is to possess multiple stable configurations of the frozen state. The interfacial layer will be in one or another among the conceivable states depending on the thermal and magnetic history. The application of a strong field, even at a temperature lower than T_g , can force the partial Co cores with a weaker anisotropy to align along the field direction, and select a another frozen spin configuration with decreasing the temperature down to 5 K. This also leads to a shift of the loops at 5 K. Our result supports this interpretation (Fig. 10). We measured the loop shift by the following procedures: the specimens were cooled in a zero field from 300 K to a temperature T_i and further cooled in $H = 20$ kOe from T_i to 5 K where the magnetic hysteresis loops were measured. Figure 10 shows the measured H_{eb} and H_c^{FC} for the sample with $d = 6$ nm prepared at $R_{O_2} = 1$ SCCM as a function of temperature T_i . $H_{eb} = 1230$ Oe for $T_i = 30$ K, being about 11.6% of the largest

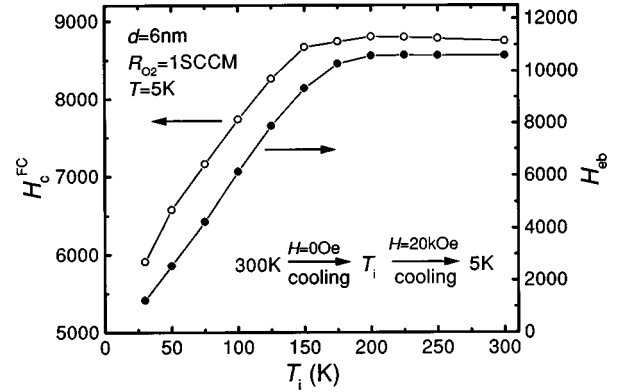


FIG. 10. H_{eb} and H_c^{FC} measured at 5 K as a function of temperature T_i , for the monodispersed Co/CoO cluster assembly with $d = 6$ nm prepared at $R_{O_2} = 1$ SCCM. T_i is the temperature where the field cooling began after being zero field cooled from 300 K.

exchange bias field ($H_{eb} = 10.6$ kOe) for $T_i > 200$ K. H_{eb} increases almost linearly with increasing T_i and then is independent of T_i for $T_i > 200$ K. This is consistent with the result of Fig. 4: H_{eb} disappears above 200 K. Moreover, as seen from Fig. 10, H_c^{FC} has the same tendency with H_{eb} when increasing T_i . This result indicates that the uniaxial anisotropy is compatible with the UEA and H_c^{FC} increases with T_i and the cooling field, which determine the amount of the Co core moments oriented in the cooling-field direction. On the other hand, the large ZFC coercivity ($H_c = 5000$ Oe) for the present Co/CoO cluster assembly with $d = 6$ nm indicates that the uniaxial anisotropy is enhanced. These results show that there are several types of FM/AF interfacial regions with different anisotropy after zero-field cooling.¹⁰ In some regions with weak anisotropy, the AF moments rotate irreversibly when the FM magnetization rotates, causing an increase of H_c . In others with strong AF anisotropy, their spins are blocked, leading to the loop shift. The presence of such a wide anisotropy distribution has been confirmed by the measurement of the magnetic relaxation (Fig. 7) where we detected the logarithmic time dependence even though a single-exponential time dependence is expected in the monodispersed Co/CoO cluster assembly.

According to the hypothesis of the spin-glass-like state in the interfacial layers between the Co core and CoO shell, moreover, the training effect (Fig. 6) can be explained reasonably as follows. The repeated magnetization reversal at high fields makes the interfacial spins change to a new frozen spin state and decreases the net interfacial uncompensated AF magnetization, causing a decrease of H_{eb} and H_c .

V. CONCLUSIONS

Using the PGC-type cluster-beam deposition technique and oxidation process under low- O_2 pressure ($< 3 \times 10^{-4}$ Torr), the monodispersed Co cluster assemblies covered by the CoO shell are obtained. The exchange bias field and coercivity strongly depend on the oxygen gas flow rate, temperature and the cluster size. H_c and H_c^{FC} increase with the increase of H_{eb} , indicating that the uniaxial anisotropy is compatible with the UEA. The result of $H_c^{FC} \approx 2H_c$ suggests that a magnetization reversal mechanism of rotation exists

and a uniaxial anisotropy is parallel to the UEA. For the monodispersed Co/CoO cluster assembly prepared at the same R_{O_2} , the sample with $d=6$ nm has the larger H_{eb} and H_c values than those with $d=13$ nm. The large ZFC coercivity ($H_c=5000$ Oe) is detected for the Co/CoO cluster assembly with $d=6$ nm. Such enhancement of H_c is attributed to irreversible magnetization reversal of the AF moments in the interfacial layers. The marked suppression of the unidirectional anisotropy above $T_v=200$ K for the present assembly is ascribed to the decrease of the anisotropy of the AF interfacial layers near the interface of the Co cores and CoO

shells and T_v is corresponding to the freezing temperature (T_g) of the spin disorder interfacial layers.

ACKNOWLEDGMENTS

This work has been supported by Core Research for Evolutional Science and Technology (CREST) of the Japan Science and Technology Corporation (JST), and partly by Grant-in-Aid for Scientific Research A1 (Grant No. 08505004). We appreciate Dr. M. Sakurai for his useful comment. We are also indebted to the support from the Laboratory for Development Research of Advanced Materials of IMR.

*Electronic address: Pengdl@imr.tohoku.ac.jp

- ¹S. Yamamuro, K. Sumiyama, M. Sakurai, and K. Suzuki, *Supramol. Sci.* **5**, 239 (1998); *J. Appl. Phys.* **85**, 483 (1999).
- ²S. Yamamuro, K. Sumiyama, T. Hihara, and K. Suzuki, *J. Phys.: Condens. Matter* **11**, 3247 (1999).
- ³D. L. Peng, K. Sumiyama, S. Yamamuro, T. Hihara, and T. J. Konno, *Appl. Phys. Lett.* **74**, 76 (1999).
- ⁴D. L. Peng, K. Sumiyama, T. J. Konno, T. Hihara, and S. Yamamuro, *Phys. Rev. B* **60**, 2093 (1999).
- ⁵W. H. Meiklejohn and C. P. Bean, *Phys. Rev.* **102**, 1413 (1956); **105**, 904 (1957).
- ⁶D. Mauri, H. C. Siegmann, P. S. Bagus, and E. Kay, *J. Appl. Phys.* **62**, 3047 (1987).
- ⁷A. P. Malozemoff, *Phys. Rev. B* **35**, 3679 (1987); *J. Appl. Phys.* **63**, 3874 (1988).
- ⁸N. C. Koon, *Phys. Rev. Lett.* **78**, 4865 (1997).
- ⁹T. C. Schulthess and W. H. Butler, *J. Appl. Phys.* **85**, 5510 (1999).
- ¹⁰C. Schlenker, S. S. P. Parkin, J. C. Scott, and K. Howard, *J. Magn. Magn. Mater.* **54-57**, 801 (1986).
- ¹¹S. Gangopadhyay, G. C. Hadjipanayis, C. M. Sorensen, and K. J. Klabunde, *Nanostruct. Mater.* **1**, 449 (1992); *J. Appl. Phys.* **73**, 6964 (1993).
- ¹²T. Ambrose and C. L. Chien, *Appl. Phys. Lett.* **65**, 1967 (1994).
- ¹³R. Jungblut, R. Coehoorn, M. T. Johnson, J. van de Stegge, and A. Reinders, *J. Appl. Phys.* **6659**, 94 (1994).
- ¹⁴J. A. Borchers, Y. Ijiri, S.-H. Lee, C. F. Majkrzak, G. P. Felcher, K. Takano, R. H. Kodama, and A. E. Berkowitz, *J. Appl. Phys.* **83**, 7219 (1998).
- ¹⁵K. Takeno, R. H. Kodama, A. E. Berkowitz, W. Cao, and G. Thomas, *Phys. Rev. Lett.* **79**, 1130 (1997).
- ¹⁶T. Ambrose, R. L. Sommer, and C. L. Chien, *Phys. Rev. B* **56**, 83 (1997).
- ¹⁷D. V. Dimitrov, S. Zhang, J. Q. Xiao, G. C. Hadjipanayis, and C. Prados, *Phys. Rev. B* **58**, 12 090 (1998).
- ¹⁸B. Dieny, V. S. Speriosu, S. S. P. Parkin, B. A. Gurney, D. R. Wilhoit, and D. Mauri, *Phys. Rev. B* **43**, 1297 (1991).
- ¹⁹B. Dieny, *J. Magn. Magn. Mater.* **136**, 335 (1994).
- ²⁰B. Barbara, C. Paulsen, L. C. Sampaio, M. Uehara, F. Fruchard, J. L. Tholence, and A. Marchand, in *Magnetic Properties of Fine Particles*, edited by J. L. Dormann and D. Fiorani (Elsevier Science, Amsterdam, 1992), p. 235.
- ²¹J. Tejada, X. X. Zhang, and E. M. Chudnovsky, *Phys. Rev. B* **47**, 14 977 (1993); J. Tejada, X. X. Zhang, and L. Balcells, *J. Appl. Phys.* **73**, 6709 (1993).
- ²²B. Barbara, L. C. Sampaio, J. E. Wegrowe, B. A. Ratnam, A. Marchand, C. Paulsen, M. A. Novak, J. L. Tholence, M. Uehara, and D. Fruchard, *J. Appl. Phys.* **73**, 6703 (1993).
- ²³J. Tejada, R. F. Ziolo, and X. X. Zhang, *Chem. Mater.* **8**, 1784 (1996).
- ²⁴P. C. E. Stamp, E. M. Chudnovsky, and B. Barbara, *Int. J. Mod. Phys. B* **6**, 1355 (1992).
- ²⁵M. Respaud, J. M. Broto, H. Rakoto, A. R. Fert, L. Thomas, B. Barbara, M. Verelst, E. Snoeck, P. Lecante, A. Mosset, J. Osuna, T. Ould Ely, C. Amiens, and B. Chaudret, *Phys. Rev. B* **57**, 2925 (1998).
- ²⁶L. Del Bianco, A. Hernando, M. Multigner, C. Prados, J. C. Sanchez-Lopez, A. Fernandez, C. F. Conde, and A. Conde, *J. Appl. Phys.* **84**, 2189 (1998).
- ²⁷K. Haneda and A. H. Morrish, *Surf. Sci.* **77**, 584 (1978).
- ²⁸S. Linderoth, S. Morup, and M. D. Bentzon, *J. Mater. Sci.* **30**, 3142 (1995).
- ²⁹L. Bel Bianco, A. Hernando, E. Bonetti, and E. Navarro, *Phys. Rev. B* **56**, 8894 (1997).
- ³⁰R. H. Kodama, A. E. Berkowitz, E. J. McNiff, and S. Foner, *Phys. Rev. Lett.* **77**, 394 (1996); *J. Appl. Phys.* **81**, 5552 (1997).